

RESEARCH

Open Access



Transcriptome-based analysis reveals relationship between duck eggshell color and eggshell strength

Longxin Wang^{1,2}, Hehe Liu³, Simeng Yu¹, Meixi Lu¹, Yunsheng Zhang¹, Shuaiqin Wang¹ and Shuisheng Hou^{1,2*}

Abstract

Background The strength of duck eggshells is essential for their storage, transportation, and processing, with various studies indicating a correlation between eggshell color and strength.

Results Our research has demonstrated that green-shelled duck eggs exhibit higher eggshell strength compared to white-shelled eggs in the M2 Line Pekin Duck population. To this end, we established mRNA transcriptome profiles of 10 eggshell gland tissues and 10 liver tissues and constructed gene expression networks in the two tissues. RNA-Seq analysis suggests that genes associated with ion transport, transmembrane transport, and liver cell proliferation and differentiation in the eggshell gland could play important roles in eggshell formation. The liver of green shell duck has stronger cell proliferation ability to maintain its homeostasis, and the eggshell gland has stronger ability to secrete eggshell matrix protein, which may be the reason why the eggshell is stronger than that of white shell duck. Through Weighted gene co-expression network analysis (WGCNA), three related modules were found in eggshell gland and liver, respectively, and three key genes were screened in each tissue (eggshell gland: *FKBP10*, *PPARG*, *MAP3K5*, liver: *PHLDA1*, *FLT3*, *CACNB4*). They have important regulatory effects on eggshell color and eggshell strength respectively.

Conclusions Through transcriptome analysis, we identified key genes associated with eggshell color (ESB) (Gland: *ABCG2*, *SLC51B*; Liver: *COX1*, *DIO3*, *RBPJ*) and eggshell strength (ESS) (Gland: *MAP3K5*, *PPARG*, *FKBP10*; Liver: *PHLDA1*, *FLT3*, *CACNB4*). We propose that these genes regulate ESB and ESS by modulating antioxidant capacity and bile acid synthesis in the liver and shell gland, leading to enhanced biliverdin deposition and stronger eggshells in green-shelled ducks. Additionally, the upregulation of ion transport, transmembrane transport, and liver cell proliferation-related genes in green-shelled ducks further supports the observed superiority in eggshell strength.

Keywords Eggshell color, Eggshell strength, WGCNA, Biliverdin, Liver

*Correspondence:

Shuisheng Hou
houss@263.net

¹Chinese Academy of Agricultural Sciences, Institute of Animal Science, Beijing, China

²College of Animal Science & Technology, Northwest A&F University, Shaan'xiYangling, China

³Farm Animal Genetic Resources Exploration and Innovation Key Laboratory of Sichuan Province, College of Animal Science and Technology, Sichuan, China



© The Author(s) 2025. **Open Access** This article is licensed under a Creative Commons Attribution-NonCommercial-NoDerivatives 4.0 International License, which permits any non-commercial use, sharing, distribution and reproduction in any medium or format, as long as you give appropriate credit to the original author(s) and the source, provide a link to the Creative Commons licence, and indicate if you modified the licensed material. You do not have permission under this licence to share adapted material derived from this article or parts of it. The images or other third party material in this article are included in the article's Creative Commons licence, unless indicated otherwise in a credit line to the material. If material is not included in the article's Creative Commons licence and your intended use is not permitted by statutory regulation or exceeds the permitted use, you will need to obtain permission directly from the copyright holder. To view a copy of this licence, visit <http://creativecommons.org/licenses/by-nc-nd/4.0/>.

Introduction

Duck eggs are the second most consumed type of eggs worldwide [1], providing a significant source of nutrition with their high protein content and essential nutrients [2]. In Asia, duck eggs are often preserved and consumed as salted eggs, which are crucial in processed egg products [3]. Eggshell colors available in the market are primarily categorized as brown, green, and white, with a noted preference for more colorful eggshells. Factors such as weight, shape index, gloss, and color significantly determine the market value of duck eggs [4]. Among these factors, color and shell strength are particularly crucial, as premium eggs are expected to have vibrant and high shell color. The integrity and strength of the eggshell are crucial for maintaining embryo viability and ensuring the freshness of table eggs. Eggs with poor shell quality experience breakage rates of around 10–15% during the handling process from laying to market, leading to increased costs [5]. Moreover, cracked eggs have a higher microbial contamination rate, with severe fractures allowing Gram-negative bacteria to thrive, posing a food safety risk [6]. Therefore, eggshell quality is a significant concern in poultry farming [7].

Research indicates a correlation between eggshell color and strength. Among different colored eggshells, green-shelled eggs generally have higher shell strength than white-shelled ones [8]. Darker eggshells, which contain more pigments [9], tend to exhibit greater strength [8, 10, 11]. Despite these findings, using color as a reliable indicator of eggshell quality remains inconclusive. Common eggshell pigments like biliverdin, producing green, and protoporphyrin, producing brown, have been identified [12–14]. *In vitro* studies have shown that biliverdin can make calcite structures rougher, thereby impeding crack propagation in the eggshell [15, 16]. Delta-aminolevulinic acid serves as a precursor to heme and can be converted into protoporphyrin within skin and liver tissues [17, 18]. Studies have suggested that adding Delta-Aminolevulinic acid to the diet can deepen eggshell color and improve shell strength [19].

The origin of biliverdin in eggshells is controversial. Biliverdin, a primary bile pigment, is predominantly synthesized in the liver, circulated systemically via the bloodstream, and partially absorbed in the small intestine. A fraction of this pigment is recirculated to the liver, while the remainder undergoes conversion into secondary bile acids by gut microbiota before fecal excretion [20]. However, emerging evidence suggests alternative mechanisms for biliverdin deposition in eggshells, including *de novo* synthesis within the uterine eggshell gland or localized production via erythrocyte phagocytosis, where heme liberated from degraded red blood cells serves as a precursor in phagocytes. Eggshell mineralization and pigment deposition are widely recognized to occur primarily

in the uterus. The eggshell gland, located in the uterine segment of the oviduct, orchestrates the coordinated release of calcium ions, bicarbonate ions, biliverdin, protoporphyrin, and specialized proteins into the uterine fluid upon egg entry [21]. These organic and inorganic components interact dynamically to form the multilayered eggshell structure [22]. The eggshell is composed of various layers, including the membrane, mammillary layer, palisade layer, crystalline layer, and cuticle, each with specific roles and structures [23], with the palisade layer's calcium carbonate crystal structure and thickness, and the mammillary layer's thickness and density determining the eggshell's strength [24]. In green-shelled eggs [25, 26], biliverdin is predominantly localized within the cuticle, where it forms stable associations with the calcium carbonate-phosphate matrix of the eggshell surface [13].

The avian eggshell gland plays a critical role in depositing pigments and minerals on the eggshell through a complex interplay of ion transport proteins and biological pathways. However, the specific mechanisms governing eggshell mineralization in ducks with varying eggshell colors remain unclear. Moreover, the liver, a key organ responsible for regulating metabolism, antioxidation, and immunity, can impact eggshell color and strength [27, 28]. This research focuses on a continuously selected population of M2 Line Beijing Ducks, a small-sized egg-laying breed known for producing white and green-shelled eggs. Through analyzing the transcriptomes of the eggshell gland and liver from duck laying eggs of different colors, we aim to identify crucial genes linked to eggshell mineralization and pigmentation while uncovering the mechanisms that connect eggshell color and strength.

Materials and methods

Ethical approval declarations

This study complies with the institutional and national guidelines regarding the breeding and use of animals. It has been approved by the Animal Experiment Committee of the Institute of Animal Sciences, Chinese Academy of Agricultural Sciences (Approval Number: IAS2022-103). All efforts have been made to minimize the suffering of the animals. When humanely killing the ducks, we placed them in a sealed container filled with carbon dioxide gas, causing them to inhale the carbon dioxide and die of asphyxiation.

Experimental design and sample collection

The M2 line of green-shelled and white-shelled female Pekin ducks used in this study was provided by the Changping Experimental Farm of the Beijing Institute of Animal Science, Chinese Academy of Agricultural Sciences. The M2 line is characterized by small-bodied

layers with white feathers, yellow bills, yellow feet, and an average female body weight of 1.99 ± 0.23 kg. Each duck was individually identified using a unique wing tag and housed separately under standardized rearing conditions, with ad libitum access to feed and water. All ducks exhibited normal egg-laying performance throughout the experimental period. A total of 200 healthy 60-week-old M2 Pekin ducks were randomly selected and divided into two groups based on eggshell color: the green-shelled group (G) and the white-shelled group (W). To ensure data consistency, eggs were collected daily at 6:00 am over 4 consecutive days, excluding those with imperfections. From each sampled duck, three eggs were retained, resulting in a final collection of 90 eggs at the conclusion of the experiment. Fifteen ducks were randomly chosen from each group, and the eggshell strength (ESS), biliverdin content (ESB), RGB values, egg quality, shape index, and mechanical properties were measured over three consecutive days (Table S1).

For RNA-seq analysis, a total of 15 ducks were used, including 9 green-shelled ducks and 6 white-shelled ducks. Each group included 5 biological replicates for sequencing of the liver and eggshell gland. Prior to sample collection, ducks were fasted and euthanized. The eggshell glands and livers were promptly dissected and flash-frozen in liquid nitrogen for subsequent RNA-seq analysis.

Eggshell color, egg quality, egg shape index, and eggshell mechanical properties

Based on the observation results, eggs were classified into green (G) and white (W) groups. Eggshell RGB values were measured using a camera under a standard light source with D65 in a lightbox (Beijing Jiu Yan Technology Co., Ltd., Beijing, China). ESB was measured according to S. et al. [29]. Specifically, eggshells were washed with water and dried in darkness. Then, 0.25 g of eggshell sample was dissolved in 4 mL of a mixed solution (methanol: concentrated HCl, volume ratio 2:1) in a plastic vial. The solution was kept in darkness for 12 h for complete pigment extraction. After centrifugation at 1300 g for 45 min, the absorbance of the supernatant was measured at 420 nm using a spectrophotometer to determine the biliverdin content in the eggshell. Standard biliverdin (2.5 mg, Shanghai Yuanye Biotechnology Co., Ltd, Shanghai, China) was dissolved in the mixed solution (2:1 methanol: concentrated HCl, volume ratio) to prepare a standard solution. The standard solution was kept in darkness until completely dissolved to construct a calibration curve for calculating the pigment concentration in samples. ESS was determined using an eggshell strength tester (EFG0503, Bulader Technology Development Co., Ltd, Beijing, China), and egg quality was measured using an integrated egg quality tester (EMT5200,

Robotmation Co., Ltd, Tokyo, Japan). For ESS measurement, the pointed end of the egg was placed vertically upwards on the table. The egg shape index was measured using a caliper with the pointed end of the egg placed horizontally upwards on the table. Eggshell thickness was measured using an eggshell thickness gauge with the cuticle layer facing upwards, and efforts were made to remove the eggshell membrane [30].

RNA isolation, library construction, sequencing, and data quality control

Liver and eggshell gland tissue samples from 10 duck specimens were stored in liquid nitrogen and used for RNA extraction via the phenol/chloroform method. RNA purity was determined with the NanoDrop 2000/8000 spectrophotometer (Thermo Fisher Scientific, Wilmington, DE, USA), while RNA concentration and integrity were assessed using the Agilent 4200 Tape Station with the Agilent RNA Screen Tape Assay (Agilent Technologies, Massy, France). RNA-Seq libraries were prepared by Annoroad Gene Technology Corporation (Beijing, China) and underwent high-throughput sequencing on the Illumina platform after passing quality control checks. Raw sequencing reads were obtained through base calling with bcl-convert, followed by filtering to remove reads with adapter contamination (>5 bp), bases with a quality score ≤ 19 representing over 50% of total bases, and reads containing more than 5% unknown nucleotides. The resulting clean reads were utilized for subsequent analyses.

Transcriptome analysis

Aligning paired-end clean reads to the duck reference genome ZJU 1.0 (GCF_015476345.1) was performed using STAR-2.7.8a. Gene counts and annotated gene information were calculated using htseq-count. Subsequently, differential expressed genes (DEGs) analysis was conducted on the Counts Per Million (CPM) normalized data using EdgeR, identifying genes with $|\log_2 \text{FoldChange}| > 1.0$ and $P\text{-value} < 0.05$ as DEGs [31]. Perform GO and KEGG enrichment analysis using the clusterProfiler package in R and visualize the results using barplot and dotplot.

WGCNA analysis

Perform WGCNA analysis using the WGCNA package in R, with CPM values as the expression matrix, filtering out genes with $\text{CPM} < 3$. The remaining genes are used to construct the co-expression network. Use the blockwiseModules function to automatically construct co-expression modules with a mergeCutHeight of 0.3 and a minModuleSize of 30 [32].

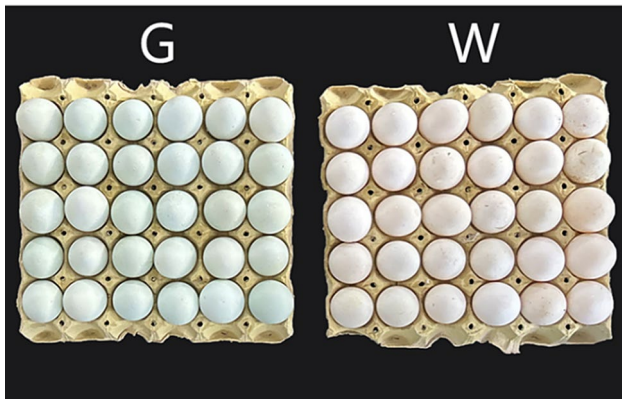


Fig. 1 Differences in eggshell color and strength between the G and W groups. The G group exhibited uniformly green eggshells, while the W group exhibited white eggshells

Quantitative PCR

Reverse Transcription - Quantitative PCR (RT-qPCR) validation was performed on the shell gland and liver tissues of the 15 samples used for RNA-Seq. Specific primers for each gene were designed using the NCBI Primer-BLAST tool (Supplementary Table S7). *GAPDH* was used as the housekeeping gene. As previously described, total RNA was extracted from the shell gland and liver using the TRIzol method. Reverse transcription was performed using the HiScript III All-in-one RT SuperMix Perfect for qPCR (Vazyme, Nanjing, China). RT-qPCR was conducted with the TB Green® Premix Ex Taq™ II FAST qPCR and the QuantStudio5 Real-Time PCR system (Thermo Fisher Scientific, Wilmington, DE, USA), with three replicates per sample. The cycling conditions were 95 °C for 30 s, followed by 40 cycles of 95 °C for 5 s and 60 °C for 10 s, with annealing and extension at 60 °C for 15 s. Melt curves were obtained for each amplification product. The $2^{-\Delta\Delta CT}$ method was used to quantify the relative changes in gene expression in the RT-qPCR experiments, normalized to *GAPDH*. Statistical analysis was conducted using t-tests in R (v. 4.2.3) [33].

Statistical analysis of data

The statistical significance of all descriptive statistical values was determined using the student's t-test. All statistical analyses and graphical plots were performed using the statistical software R (v. 4.2.3). Results of basic descriptive statistics are presented as mean and standard deviation (Mean ± SD) in the text and tables.

Results

Phenotypic statistics of green-shelled and white-shelled eggs

The egg color difference between the G group and the W group was found to be statistically significant (Fig. 1).

Table 1 Average unit biliverdin concentration and RGB value

Group	G	W	P value
Eggshell biliverdin(mg/ml)	0.03 ± 0.002 ^a	0.02 ± 0.003 ^b	< 0.001
R value	195.76 ± 19.332 ^b	210.69 ± 9.254 ^a	0.012
G value	189.59 ± 19.084 ^b	205.73 ± 10.746 ^a	0.008
B value	189.54 ± 19.079 ^b	207.63 ± 9.971 ^a	0.003

^{a, b} For each index, means with no common superscript differ significantly at $P < 0.05$

Table 2 Phenotypic statistics of egg quality traits

Group	G	W	P value
Egg shape index	1.42 ± 0.036	1.40 ± 0.026	0.151
Yolk color	3.62 ± 0.353	3.60 ± 0.382	0.870
Albumen height	6.30 ± 0.635	6.35 ± 0.522	0.842
Weight (g)	84.87 ± 2.113	85.36 ± 0.2443	0.563
Haugh unit	69.41 ± 6.762	36.92 ± 15.788	0.811
Eggshell strength (kg/cm ²)	4.76 ± 0.334 ^a	4.21 ± 0.415 ^b	< 0.001

^{a, b} For each index, means with no common superscript differ significantly at $P < 0.05$

Table 1 presents the biliverdin content and RGB values of the eggshells. The G group exhibited a significantly higher eggshell biliverdin compared to the W group ($P < 0.01$), along with lower R, G, and B values ($P < 0.01$). Moreover, the ESS in the G group was notably higher than in the W group ($P < 0.01$), while no significant differences were observed in other parameters (Table 2).

Differential gene expression in shell gland and liver between green-shelled and white-shelled eggs

After filtering the raw sequences, each shell gland sample library obtained over 44 million clean reads. The GC content ranged from 52.62 to 56.91% across all samples. The percentage of Q30 bases exceeded 94.06% in each group, with no significant differences in quality metrics between groups ($P > 0.05$) (Supplementary Table S2). Subsequently, the quality-controlled clean reads were mapped to the duck reference genome (GCA_015476345.1), with an average mapping rate of >75% for unique genes in the G group and >77% in the W group (Supplementary Table S3). Differential analysis was performed after filtering out genes with average expression < 1, resulting in a total of 1, 112 DEGs. Among all DEGs, compared to the G group, the W group showed significant downregulation of 651 genes and upregulation of 461 genes (Fig. 2A). The expression patterns of the top 100 significant DEGs, ranked by FDR, are illustrated in Fig. 2B, where samples from the same group cluster together between the G and W groups.

Similarly, after quality control, each liver sample was aligned to the duck reference genome (GCA_015476345.1) with an average mapping rate of 84.34% (Supplementary Table S3). After filtering out

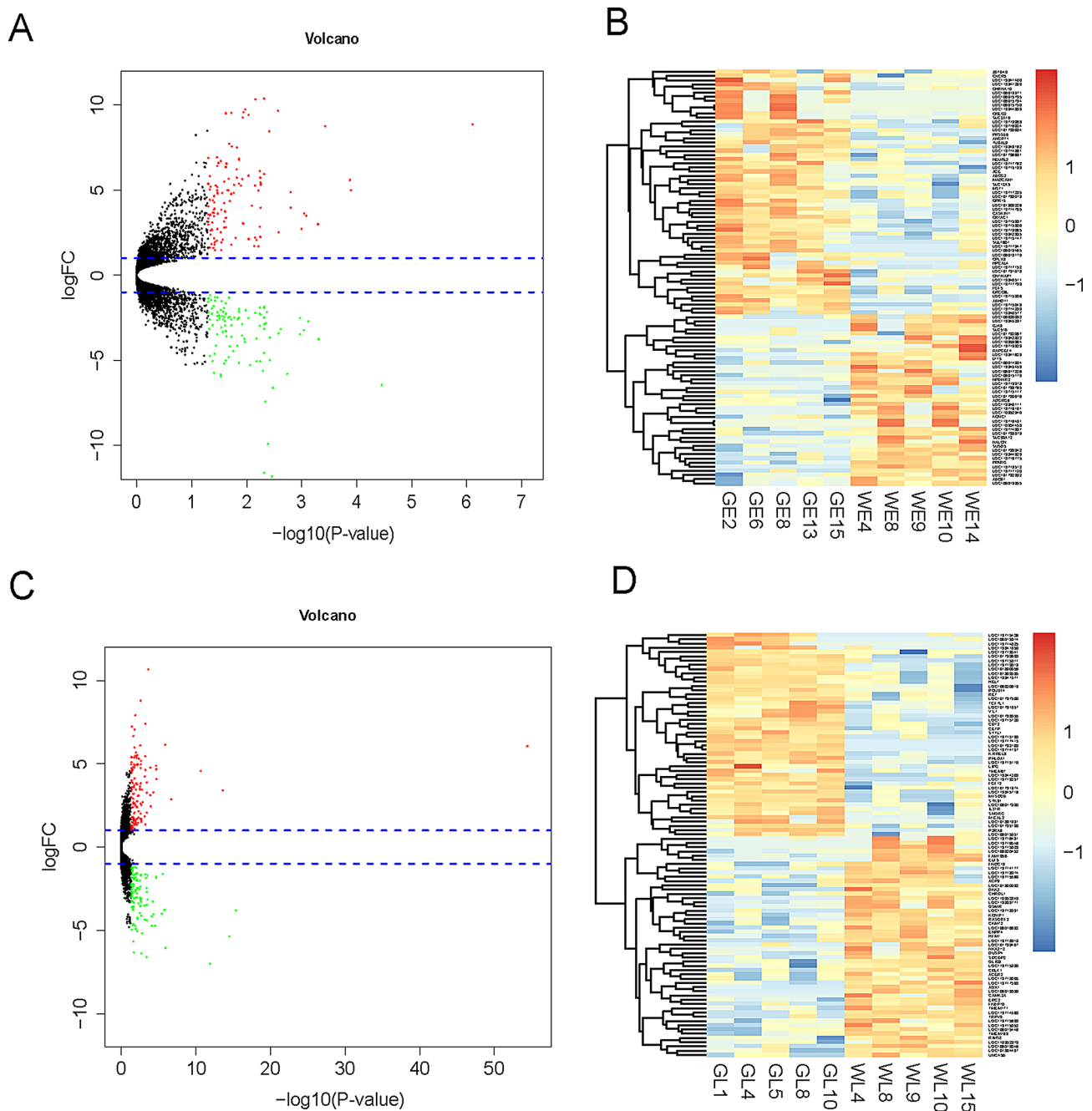


Fig. 2 Identification of DEGs in the shell gland and liver between green and white shelled groups. **A)** Volcano plot of DEGs in the shell gland. **(B)** Heatmap of the top 100 DEGs in the shell gland, sorted by FDR. **(C)** Volcano plot of DEGs in the liver. **(D)** Heatmap of the top 100 DEGs in the liver, sorted by FDR

genes with average expression < 1 , the differential analysis identified 1078 DEGs, with 535 genes downregulated and 543 genes upregulated (Fig. 2C, D).

Differential gene functional annotation and pathway enrichment in shell gland and liver

Through Gene Ontology (GO) term enrichment and Kyoto Encyclopedia of Genes and Genomes (KEGG) pathway enrichment, we gained insights into the

functions of differential genes. In the shell gland, a total of 20 GO terms and 1 KEGG pathway were significantly enriched ($p_{\text{adjust}} < 0.05$; Supplementary Table S4, S5), primarily classified into two categories. Biological processes were mainly related to the development and regulation of substance metabolism, including positive regulation of epithelial cell migration, animal organ development, small molecule metabolic processes, and carbohydrate metabolic processes. Molecular functions

were associated with substance transport, ion channel activity, and glycoprotein binding, involving activities such as neurotransmitter receptor activity involved in the regulation of postsynaptic membrane potential, excitatory extracellular ligand-gated ion channel activity, passive transmembrane transporter activity, and glycoprotein binding. No cellular component terms were significantly enriched (Fig. 3A). In terms of pathway enrichment, differential genes were observed in signaling molecules and interaction pathways, notably with the Calcium signaling pathway ranking second, albeit not significantly ($P < 0.01$, $p.adjust > 0.05$) (Fig. 3B).

In the liver, a total of 22 GO terms and 1 KEGG pathway were significantly enriched ($p.adjust < 0.05$; Table Supplementary S4), primarily associated with cell proliferation and differentiation, ion channel activity, and transmembrane transport (Fig. 3C). In the KEGG enrichment results, significant enrichment was observed in the Neuroactive ligand-receptor interaction pathway ($P < 0.01$, $p.adjust < 0.01$), followed by the Calcium signaling pathway and Melanogenesis ($P < 0.01$, $p.adjust > 0.05$).

Eggshell biliverdin content and eggshell strength co-expressed gene modules

After filtering the gene expression matrix of ten individuals' shell gland tissues for genes with CPM values greater than 3, 11, 758 genes remained. A gene co-expression clustering dendrogram was constructed, and using all samples, an unsigned network was built with a soft threshold of 17 ($\beta = 17$), achieving a scale-free topology fitting index $R^2 > 0.90$. All genes are clustered into 14 modules (Fig. 4A), with varying numbers of genes per module ranging from 41 to 4845 (Fig. 4B). To identify key modules associated with ESB and ESS, further analysis of module-phenotype relationships was conducted (Fig. 4C). Three modules showed high correlation with ESB and ESS: the green module had correlations of 0.81 ($P < 0.01$) with ESB and 0.56 ($P = 0.09$) with ESS, the brown module had correlations of -0.77 ($P = 0.01$) with ESB and -0.72 ($P = 0.02$) with ESS, and the red module had correlations of -0.73 ($P = 0.02$) with ESB and -0.63 ($P = 0.05$) with ESS (Fig. 4C).

Similarly, after filtering the gene expression matrix of liver samples for genes with CPM values greater than 3, 12, 208 genes remained. A gene co-expression clustering

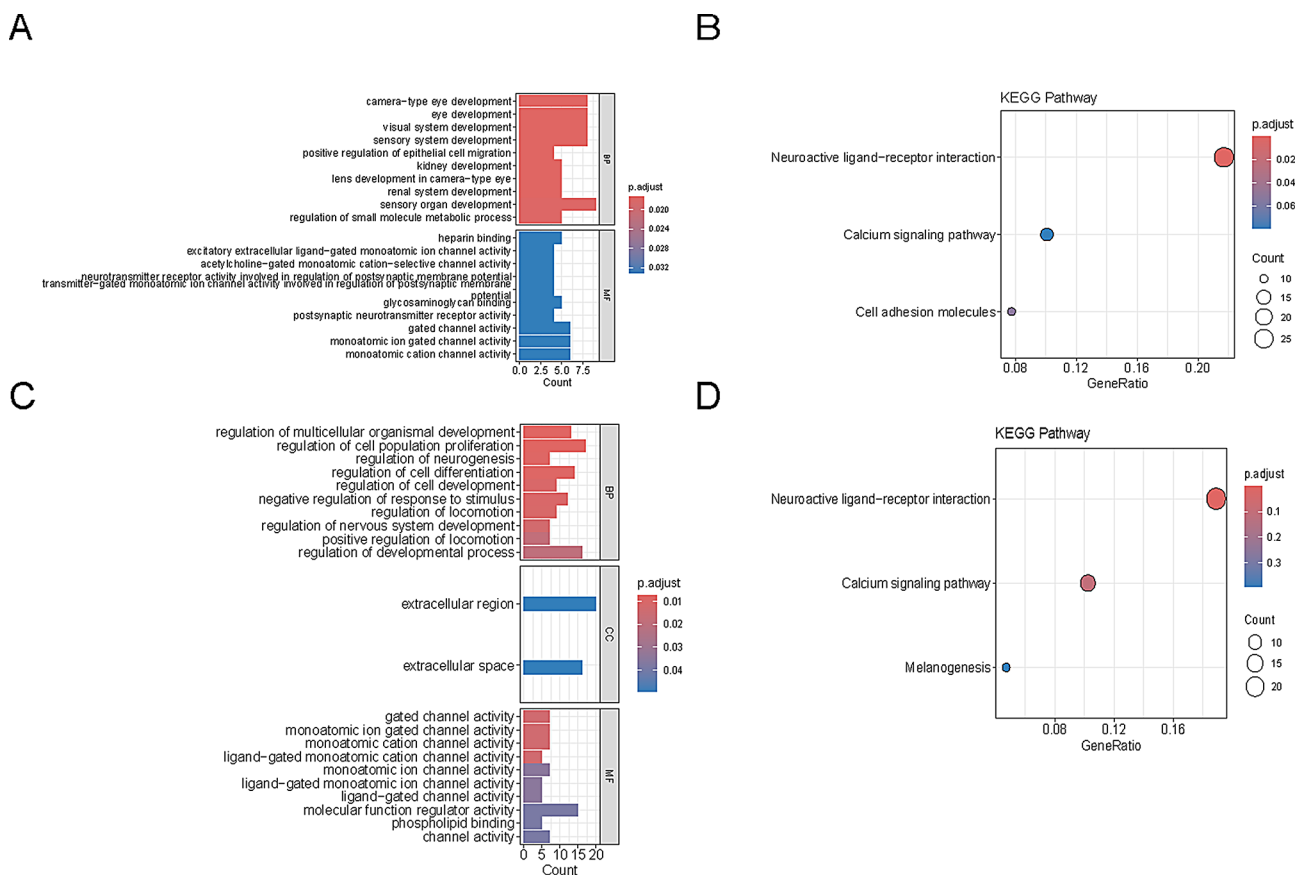


Fig. 3 Functional and Pathway Enrichment of DEGs in Shell Gland and Liver between G and W Groups. **(A)** Barplot of GO Enrichment of DEGs in Shell Gland. **(B)** Bubble Plot of KEGG Enrichment of DEGs in Shell Gland. **(C)** Barplot of GO Enrichment of DEGs in Liver. **(D)** Bubble Plot of KEGG Enrichment of DEGs in Liver

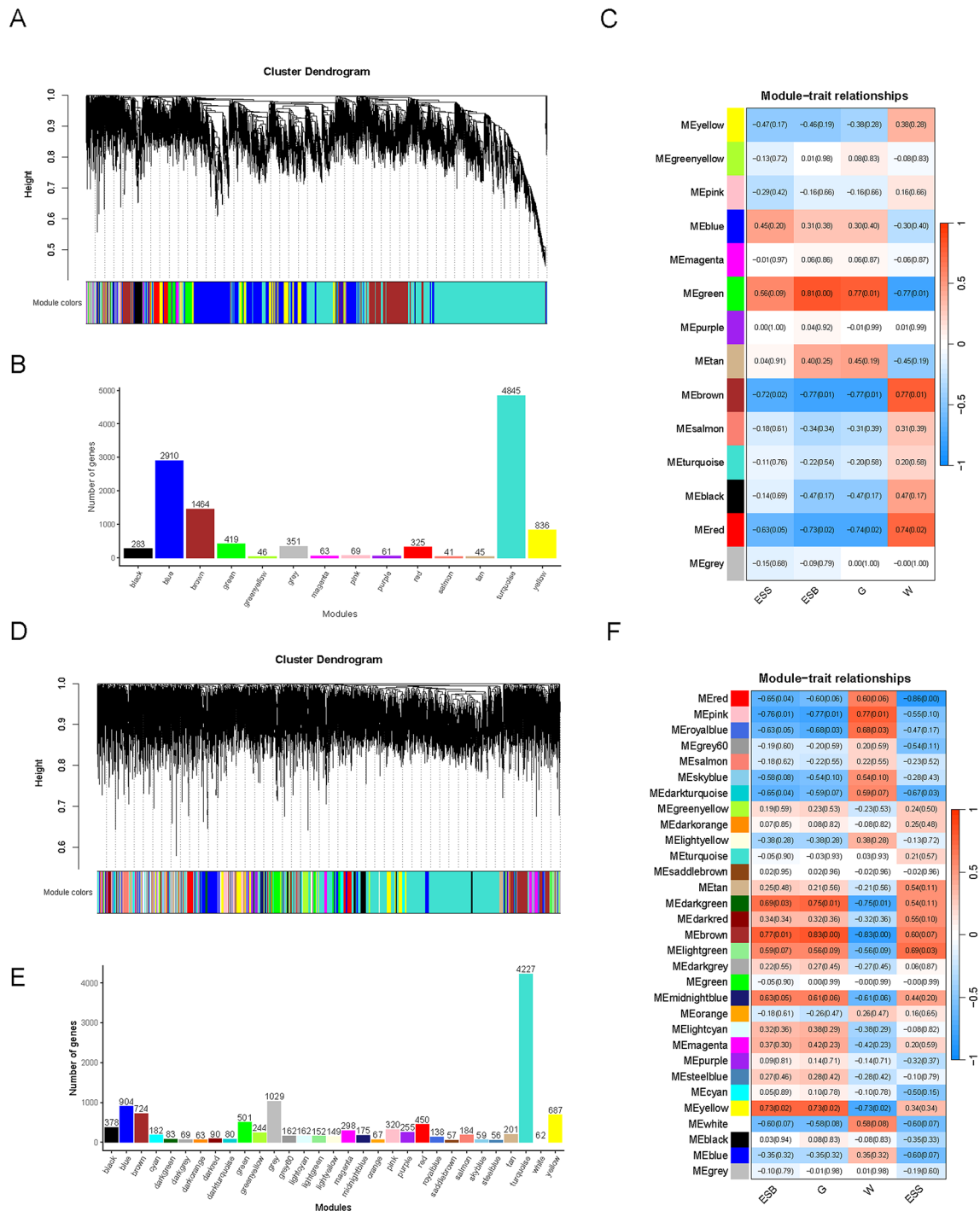


Fig. 4 Key modules and phenotype correlation matrix in eggshell gland and liver WGCNA. (A) Hierarchical clustering tree and corresponding module plot of eggshell gland genes. (B) Number of genes corresponding to each gene module. (C) Correlation matrix between each module and phenotype. (D) Hierarchical clustering tree of liver genes and corresponding module heatmap. (E) Number of genes corresponding to each gene module. (F) Correlation matrix between each module and phenotype

dendrogram was constructed with a soft threshold of 20 ($\beta=20$), resulting in all genes clustering into 31 modules (Fig. 4D). The number of genes per module varied widely, ranging from 56 to 4, 227 (Fig. 4E). Subsequently, further analysis of module-phenotype relationships was

conducted (Fig. 4F). Three modules showed a high correlation with ESB and ESS: the dark green module (ESB: 0.69, $P=0.03$; ESS: 0.54, $P=0.11$), brown module (ESB: 0.77, $P=0.01$; ESS: 0.60, $P=0.07$), and light green module (ESB: 0.59, $P=0.07$; ESS: 0.69, $P=0.03$) (Fig. 4F).

After intersecting DEGs and key modules, we identified three key modules (green, brown, and red) related to ESB and ESS in the shell gland. Additionally, we identified 14 crucial genes known for their functions (*FKBP10*,

MAP3K5, *PPARG*, *ADAMTS14*, *CHGB*, *CTRL*, *FGF2*, *MST1*, *NFASC*, *TMEM61*, *ABCB1*, *CEP170*, *DIO3*, *PGC*) (Fig. 5A, Supplementary Table S6). Functional enrichment and KEGG pathway analysis revealed significant

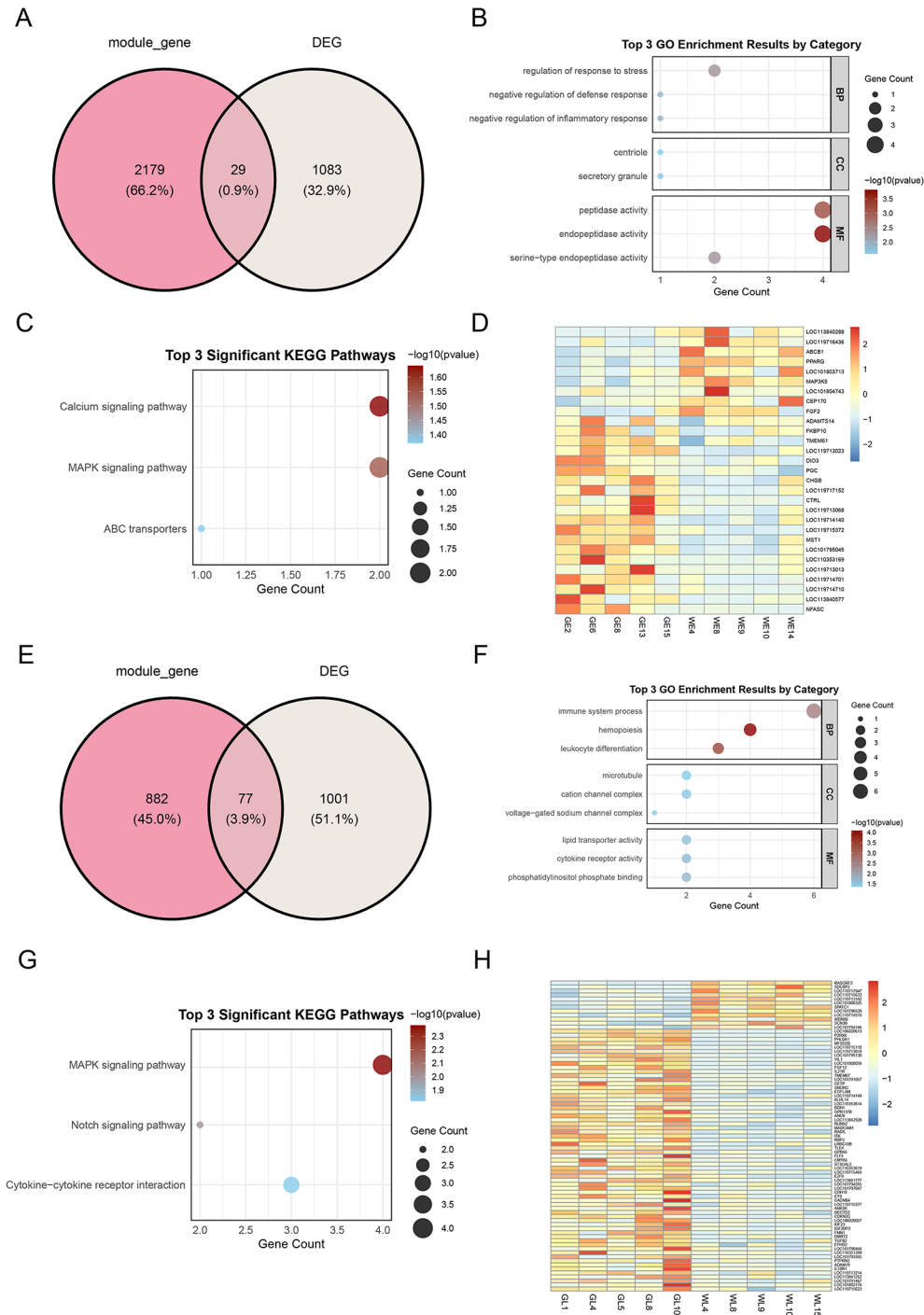


Fig. 5 Candidate gene enrichment, functional annotation, and expression patterns in shell gland and liver. **(A)** Venn diagram of genes shared between DEGs and genes in three key modules in shell gland. **(B)** Bar plot of GO enrichment of shared genes in the shell gland. **(C)** Bubble plot of KEGG enrichment of shared genes in the shell gland. **(D)** Expression patterns of shared genes in the shell gland. **(E)** Venn diagram of genes shared between DEGs and genes in three key modules in liver. **(F)** Bar plot of GO enrichment of shared genes in the liver. **(G)** Bubble plot of KEGG enrichment of shared genes in the liver. **(H)** Expression patterns of shared genes in the liver

enrichment of GO terms in cell adhesion molecule binding (MF), with KEGG pathways such as the Calcium signaling pathway and MAPK signaling pathway prominently enriched (Fig. 5B, C). The expression patterns of shared genes are depicted in Fig. 5D.

In the liver, we similarly identified three key modules (dark green, brown, and light green) associated with eggshell color and strength. Additionally, we identified 42 crucial genes known for their functions (Fig. 5E, Supplementary Table S6). Functional enrichment and KEGG pathway analysis showed that GO enrichment was predominantly related to cell migration processes, while KEGG pathways such as MAPK signaling pathway, Cytokine-cytokine receptor interaction, and Notch signaling pathway were prominently enriched (Fig. 5F, G). The expression patterns of shared genes are depicted in Fig. 5H.

Hub genes for eggshell biliverdin and eggshell strength

In each module, genes with a connectivity value based on the characteristic gene Epigengene- based connectivity > 0.5 and a topological overlap measure > 0.2 were considered hub genes. The expression network of the shared genes was visualized using Cytoscape software. The results showed that in the eggshell gland, *CEP170* and

NFASC were identified as key genes related to eggshell color and strength (Fig. 6A). In the liver, *SNORC*, *ANKS6*, *EGFLAM*, *IGF2BP3*, *IL18R1*, and *KIF23* were identified as key genes related to eggshell color and strength (Fig. 6B).

RT-qPCR validation of differential expressed genes

To verify the accuracy of RNA-seq, we chose to validate hub genes and important DEGs. The results showed that the expression trend of hub genes and important DEGs was the same as that of RNA-seq (Fig. 7).

Discussion

The ESS is primarily influenced by maternal biomineralization capacity (genetics, age), nutrition, and husbandry practices [34, 35], and it shows a correlation with eggshell color [8, 36]. In 2006, Schreiweis et al. identified QTLs related to eggshell mass and color on chromosome 4 [37], and in 2007, Mróz et al. reported that eggshells with noticeable pigment spots tend to have thicker crystal layers and membranes [38]. In our study, we also observed significant differences in ESS associated with eggshell color; within the same strain, green-shelled eggs exhibit stronger shells compared to white-shelled eggs, consistent with previous findings [8, 10]. However, there is inconsistency regarding the relationship between

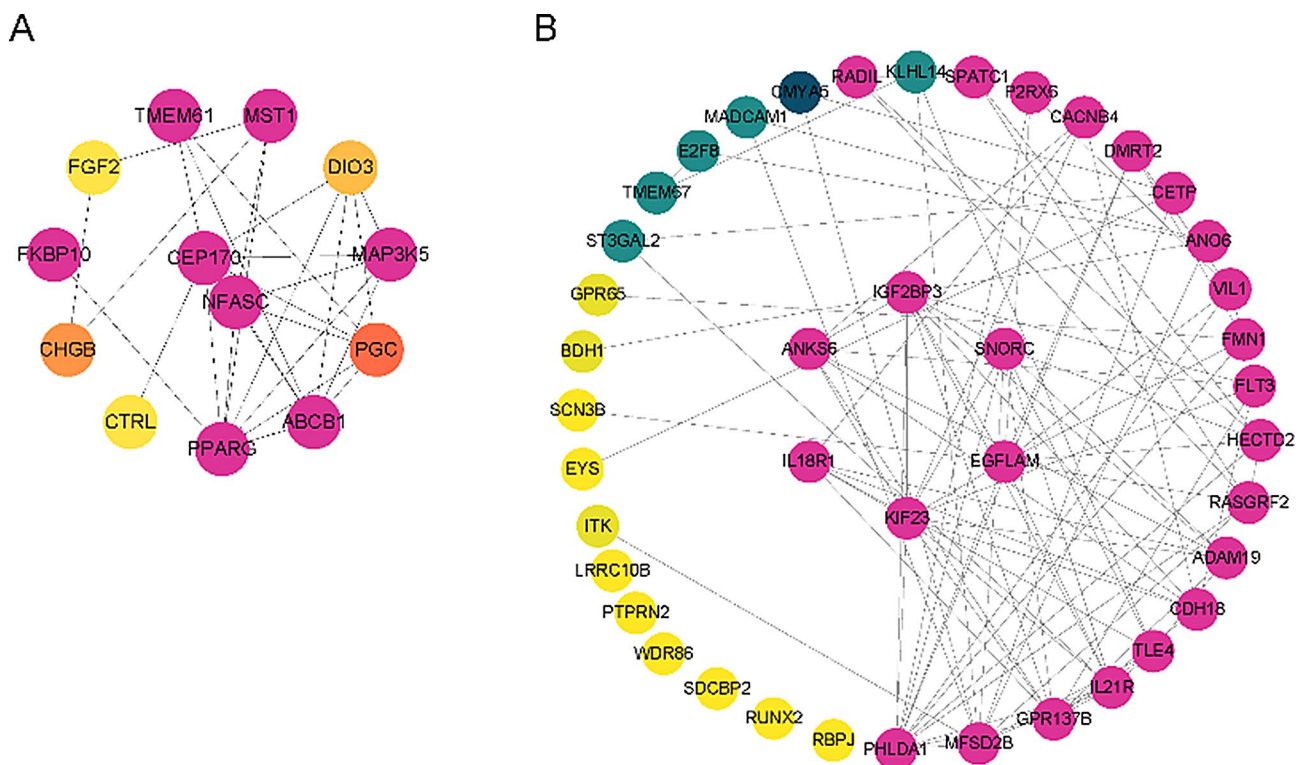


Fig. 6 Expression networks of candidate genes. **(A)** Expression network of candidate genes in the eggshell gland. The pinker the color, the higher the connectivity of the gene in the network, and the yellower the color, the lower the connectivity of the gene in the network. The center of the circle is the hub gene. **(B)** Expression network of candidate genes in the liver. The pinker the color, the higher the connectivity of the gene in the network, and the yellower the color, the lower the connectivity of the gene in the network. The center of the circle is the hub gene

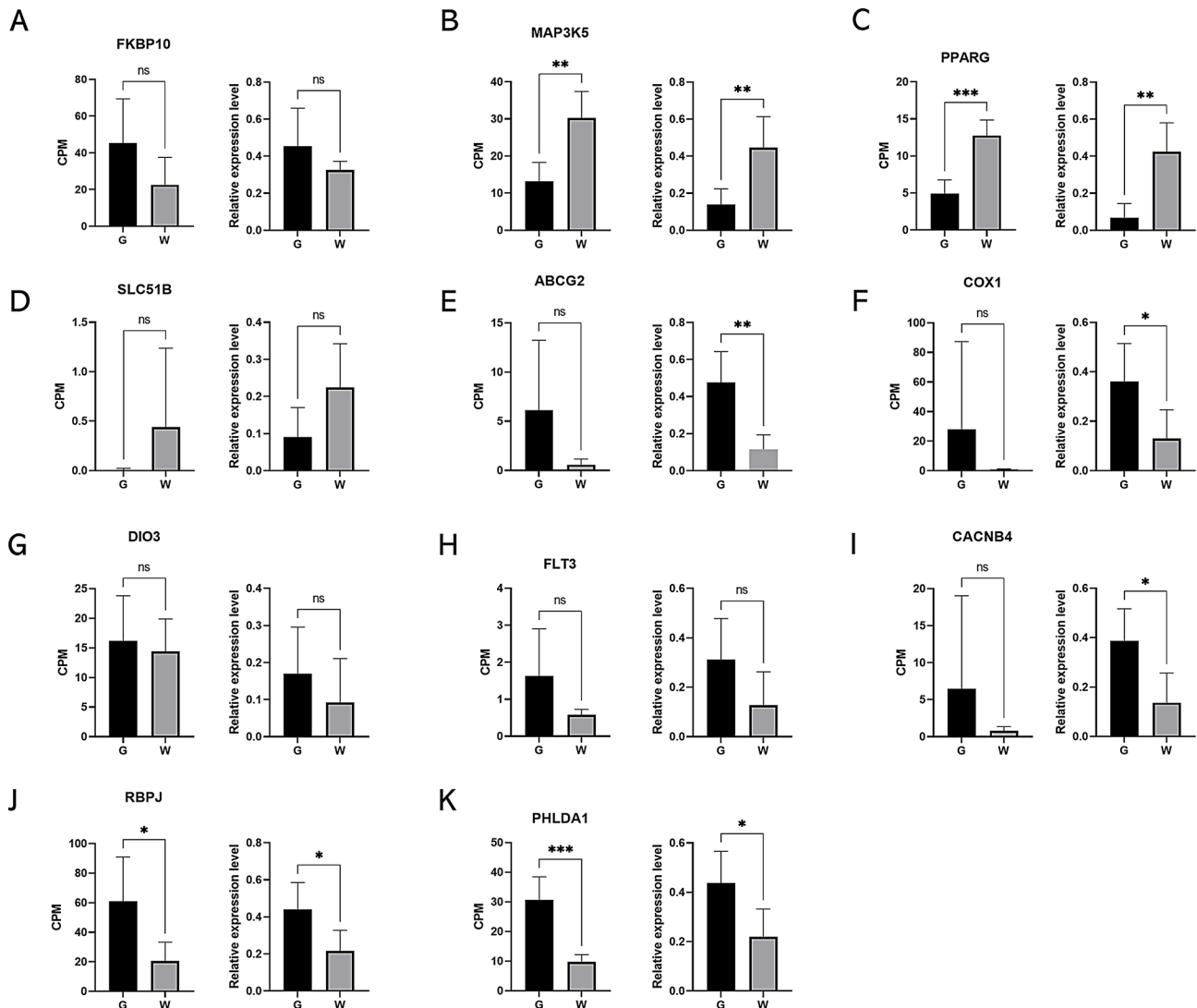


Fig. 7 RT-qPCR validation of RNA-seq results

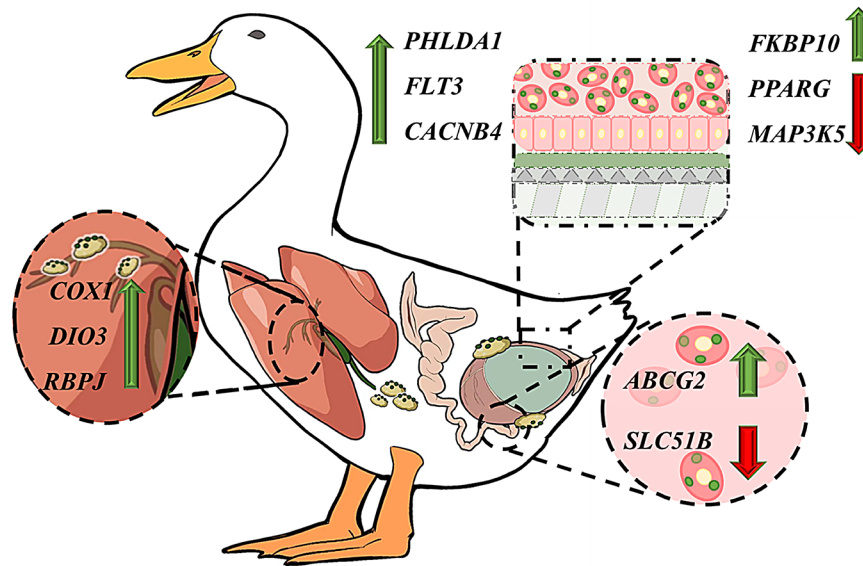
eggshell color and eggshell quality [11, 39]. Therefore, whether eggshell color can serve as an indicator of ESS requires further investigation. One potential reason for the conflicting results is the lack of molecular mechanism information, such as genes and pathways related to eggshell quality in the shell gland and liver of green and white shell ducks. Therefore, in subsequent studies, we analyzed the DEG and eggshell phenotype co-expression network between white-shelled duck and green-shelled duck based on transcriptome.

Our transcriptome analysis of the liver and shell gland revealed several genes associated with ESB (Gland: *ABCG2*, *SLC51B*; Liver: *COX1*, *DIO3*, *RBPJ*), and ESS (Gland: *MAP3K5*, *PPARG*, *FKBP10*; Liver: *PHLDA1*, *FLT3*, *CACNB4*). Based on gene co-expression patterns and functional annotations, we hypothesize that the liver and shell gland may coordinately regulate eggshell traits through bile acid metabolism, antioxidant capacity, and

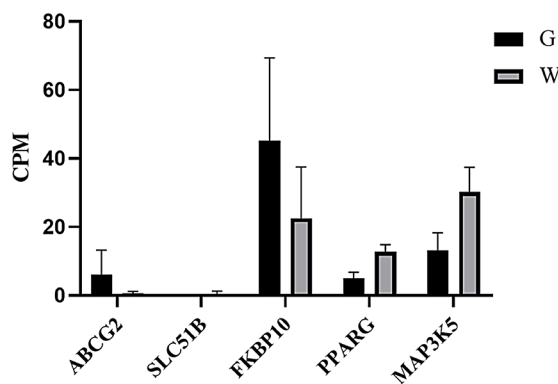
ion transport pathways (Fig. 8). However, this hypothesis requires further functional validation.

Previous research has identified *ABCG2* as a causal gene for green eggshells [14, 40]. *ABCG2* is a multidrug membrane transporter protein transporting various endogenous and exogenous substances. It is responsible for renal excretion of urate, mitigating tissue oxidative stress, and inflammatory responses [41, 42]. Furthermore, *ABCG2* can also transport protoporphyrin and heme, potentially contributing to biliverdin production. In this study, *ABCG2* expression was significantly upregulated in the shell gland of green-shelled ducks, supporting its significant role in green eggshell coloration. Additionally, *SLC51B* is an organic solute transporter protein involved in bile acid reabsorption [43]. *SLC51B* can export bile acids to the basolateral membrane, preventing bile accumulation. Bile acids contribute to biliverdin secretion, and the significant upregulation of *SLC51B* in the shell

A



B



C

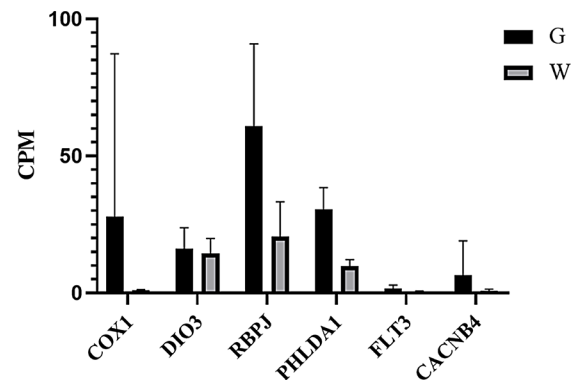


Fig. 8 Proposed Synthesis, Transport Mechanism of Biliverdin, and Formation of Harder Eggshells in Green-Shelled Ducks' Liver and Eggshell Gland. **(A)** A schematic illustrating the hypothesized synthesis and transport of biliverdin in the liver and eggshell gland of green-shelled ducks. Free heme in the liver is thought to bind to *COX1*, thereby activating cytochrome c oxidase activity and regulating intracellular oxidative stress. The joint regulation of bile homeostasis by *DIO3* and *RBPJ* is proposed to facilitate the excretion of bile acids into the circulatory system. These bile acids are then absorbed by the eggshell gland, where high expression of *ABCG2* is observed. It is hypothesized that biliverdin is subsequently separated and contributes to the green coloration of the eggshell. Decreased expression of *SLC51B* may inhibit the transport of biliverdin out of the eggshell gland, thereby promoting the green eggshell phenotype. Additionally, upregulated expression of *PHLDA1*, *FLT3*, and *CACNB4* in the liver may support liver cell proliferation and homeostasis. In the eggshell gland, increased *FKBP10* expression is proposed to assist protein folding, contributing to the formation of a stronger eggshell matrix. **(B)** CPM values of ESB key genes in eggshell gland and liver. **(C)** CPM values of ESB key genes in eggshell gland and liver

gland of white-shelled eggs may increase bile acid output, potentially reducing the gland's ability to secrete biliverdin compared to green-shelled eggs. Reported pigments are all precursors or derivatives of biliverdin [44]. The pathways related to heme involve both heme synthesis and heme detoxification. In the synthesis pathway, porphyrin serves as the penultimate product, while in the breakdown pathway, biliverdin is the first product, followed by bilirubin and urobilinogen [45–48]. Liver is the

active site for heme biosynthesis, where the intermediate products of this pathway are essential for the function of hepatic hemoglobin, particularly within the cytochrome P450 system [49], *COX1* is the core subunit of cytochrome c oxidase [50], it contributes to the activity of cytochrome c oxidase. When heme and cofactors are inserted into its subunits, it becomes active. Cytochrome c, a rate-limiting enzyme in the mitochondrial respiratory chain, helps regulate intracellular oxidative stress [51].

DIO2 contributes to bile acid homeostasis in the liver [52], it also regulates mitochondrial function to counteract cellular oxidative stress [53]. *RBPJ* is a transcriptional regulator involved in Notch signaling, its high expression can promote bile duct maturation, and increase liver bile flow, thereby facilitating significant bile acid output, and preventing bile acid accumulation in the liver [54]. We hypothesize that the high expression of *DIO2* and *RBPJ* in Group G will collectively promote the excretion of bile acids from the liver into circulation, thereby influencing the color of the eggshell [28]. It is also believed that the liver regulates eggshell color, with female birds producing deeper, green-shelled eggs exhibiting stronger bile acid synthesis and antioxidant capabilities. Bile acids synthesized by the liver enter the circulatory system and are subsequently absorbed by the shell gland to synthesize eggshell pigments [44]. Based on these findings, this study suggests that the liver of green-shelled female ducks exhibits stronger antioxidant capacity and bile acid synthesis capability. Simultaneously, the shell gland of green-shelled eggs demonstrates enhanced bile acid absorption ability, which contributes to the deposition of biliverdin in the eggshell.

The shell gland is the site for eggshell mineralization and pigment deposition, and it regulates tissue homeostasis, cell proliferation, and apoptosis [35, 55]. The regulation of extracellular proteins and ion transport proteins plays a significant role in the secretion, transport, and binding of minerals, influencing both ESS and pigment deposition through various cellular and molecular processes [56–58]. In the enrichment analysis, GO and KEGG pathway analysis predominantly enriched for transmembrane transporter activity, ion channel regulation activity, glycosaminoglycan synthesis, and calcium signaling pathway. This is consistent with the findings reported by Jonchère et al., who states that the genes associated with high ESS in the shell gland are mostly related to ion transport [10]. The eggshell matrix is formed through interactions between calcium carbonate and proteins. The shell gland exhibits active ion transport, where various secretory proteins secrete calcium carbonate and proteins into the uterine fluid undergoing mineralization. Protein fold and aggregate along with calcium deposition. Under the contraction and movement of the shell gland, the egg rotates, facilitating calcification and eventual expulsion [10, 59]. In the transcriptome results, the upregulation of genes related to ion transport pathways in Group G may be critical for high ESS. Additionally, glycosaminoglycan binding function contributes significantly to ESS. Glycosaminoglycans are important components of eggshell and eggshell membrane, playing a role in biomineralization, and their levels show a significant correlation with ESS [60].

WGCNA analysis highlights the pivotal role of the shell gland's material transport capacity in determining eggshell color and mechanical strength. In avian species, precursors of the eggshell matrix are transported from the bloodstream to the shell gland via epithelial cells, where the morphological integrity of the glandular endometrium critically regulates ion absorption and matrix deposition [61]. Aging or pathological conditions in laying hens can induce structural damage to the shell gland, impairing ion transport (e.g., Ca^{2+}) and disrupting crystallization processes, ultimately leading to reduced eggshell quality and pigmentation defects [35, 39, 62]. Notably, the shell gland exhibits heightened sensitivity to apoptosis and tissue damage during calcification, with such damage directly restricting Ca^{2+} mobilization and diminishing eggshell strength (ESS) [63]. For instance, infectious bronchitis virus (IBV) infections compromise shell color by targeting oviductal epithelial cells, downregulating type I collagen and calcium-binding protein 28 kDa, and thereby inhibiting mineralization and pigment deposition [39]. These findings collectively underscore the importance of collagen dynamics and apoptosis regulation in shell gland function. In this study, *MAP3K5* and *PPARG* were significantly upregulated in the shell gland of white-shell laying hens compared to green-shell hens (Fig. 8B). *MAP3K5*, a redox-sensitive serine/threonine kinase, serves as a marker for ferroptosis and triggers apoptosis through JNK/p38 signaling pathways [64, 65]. *PPARG*, a nuclear receptor involved in peroxisome proliferator-activated receptor signaling, further modulates apoptotic cascades [66]. Their elevated expression in the white-shell group suggests enhanced apoptosis in the shell gland epithelium, consistent with prior reports linking oxidative stress to glandular dysfunction, reduced cell viability, and eggshell discoloration [67]. This apoptotic activation likely disrupts Ca^{2+} transport and matrix organization, contributing to the inferior shell quality observed in white-shell eggs. Conversely, *FKBP10*, encoding a member of the FKBP peptidyl-prolyl cis-trans isomerase (PPIase) family, was markedly downregulated in white-shell hens. *FKBP10* facilitates collagen maturation and cross-linking, processes essential for bone mineralization and crystal growth [68, 69]. The decreased expression of *FKBP10* may reduce collagen maturation and cross-linking, thereby inhibiting mineralization and pigmentation of the eggshell. Its deficiency has been linked to defective mineralization and abnormal bone architecture, paralleling our observation of impaired eggshell calcification in the white-shell group. Intriguingly, Gene Ontology annotation identifies *FKBP10* as a calcium ion-binding protein, and its higher expression in green-shell hens implies superior calcium-binding capacity within the shell gland. This enhanced Ca^{2+} sequestration likely promotes matrix mineralization and structural

reinforcement, explaining the improved mechanical strength and pigmentation stability of green-shell eggs. These key genes are highly connected with hub genes (*CEP170* and *NFASC*) (Fig. 7A). The product of *CEP170* is a component of the centromere and plays an important role in cell division [70]. *NFASC* is a protein that connects the extracellular matrix of the axon initial segment to the intracellular cytoskeleton [71]. Both hub genes are involved in multiple cellular processes and further regulate key genes by regulating cellular processes in the eggshell gland co-expression network.

As a multifunctional metabolic organ, the liver plays a crucial role in bile production and maintaining normal metabolism. It is also essential for egg production. With increasing age, decreased liver cell proliferation and increased apoptosis are important factors affecting the critical metabolic functions of the liver [72, 73]. In this study, the upregulation of genes involved in cell proliferation regulation (e.g., *PHLDA1*, *FLT3*, *CACNB4*) may contribute to maintaining hepatic cellular homeostasis [27, 74]. The stability of hepatocyte proliferation and metabolism, as well as the liver's lipid metabolism capacity, are believed to influence eggshell strength (ESS) by modulating the availability of calcium and other essential substrates for shell formation. The MAPK signaling pathway, identified through WGCNA, plays a central role in regulating hepatic glucose metabolism, lipid metabolism, and inflammatory responses. Within this pathway, *PHLDA1* acts as an upstream regulator that suppresses hepatic inflammation [75], while *FLT3*—a tyrosine-protein kinase—promotes dendritic cell differentiation, proliferation, and survival [76]. Notably, *FLT3* overexpression has been shown to alleviate liver cell damage and reduce hepatocyte apoptosis. Furthermore, *FLT3* can activate RAS signaling and downstream kinase phosphorylation (including MAPK1/ERK2 and/or MAPK3/ERK1), suggesting that both *FLT3* and *PHLDA1* may exert their effects through the MAPK signaling pathway. This is supported by our liver co-expression network analysis, which revealed strong connectivity between these genes and hub genes within the network. Among the highly connected genes in the network, *CACNB4* mediates calcium ion influx, modulates calcium channel voltage, and regulates gene transcription. Additionally, *CACNB4* exhibits protein kinase-binding properties [77], further implicating its role in signal transduction. As a highly connected gene in the network, *CACNB4* may regulate calcium channel activity to fine-tune transcriptional responses [78], thereby contributing to hepatic metabolic stability. Collectively, these findings suggest that the upregulation of MAPK signaling pathway-related genes (*PHLDA1*, *FLT3*, *CACNB4*) in G-group female ducks sustains hepatocyte proliferation, mitigates apoptosis, and maintains liver homeostasis. This, in turn, may enhance the liver's

capacity to support ESS by ensuring the availability of critical metabolites for eggshell formation.

Conclusions

This study conducted a comparative transcriptome analysis of shell glands and livers between white-shell and green-shell ducks and constructed co-expression networks of genes related to eggshell color and strength using WGCNA. Differential analysis identified bile acid output-related genes in the shell gland (*ABCG2*, *SLC51B*) and liver (*COX1*, *DIO3*, *RBP1*). GO, and KEGG analysis results indicated that genes related to ion transport, transmembrane transport in shell glands, and cell proliferation and differentiation in the liver may play important roles in eggshell formation. WGCNA analysis identified key modules and genes associated with eggshell color and strength. Additionally, ESS-related genes such as *MAP3K5*, *PPARG*, *FKBP10*, *PHLDA1*, *FLT3*, and *CACNB4* were identified, highlighting the critical roles of apoptosis regulation, collagen maturation, and calcium transport in shell gland mineralization. Based on these findings, we hypothesize a potential liver-shell gland interaction that may coordinate ESB and ESS through bile acid metabolism, antioxidant capacity, and ion transport pathways. However, further functional validation is required to confirm this model. This model provides molecular insights into the correlation between eggshell color and strength, offering novel targets for future research to enhance eggshell quality in poultry breeding.

Abbreviations

WGCNA	Weighted Gene Co-Expression Network Analysis
RT-qPCR	Reverse Transcription - Quantitative PCR
GO	Gene Ontology
KEGG	Kyoto Encyclopedia of Genes and Genomes
ESS	Eggshell Strength
ESB	Eggshell Biliverdin
G	Green
W	White
DEGs	Differential Expressed Genes
CPM	Counts Per Million

Supplementary Information

The online version contains supplementary material available at <https://doi.org/10.1186/s12864-025-11452-w>.

Supplementary Material 1

Acknowledgements

Not applicable.

Author contributions

L. W.: Writing—review & editing, Writing—original draft, Visualization, Formal analysis. H. L.: Writing—review & editing, Supervision, Methodology, Conceptualization. S. Y.: Writing—review & editing. M. L.: Data curation. Y. Z.: Writing—review & editing, Supervision, Resources, Investigation. S. W.: Writing—review & editing, Supervision, Resources, Investigation. S. H.: Resources, Project administration, Investigation, Funding acquisition, Conceptualization.

Funding

This study was supported by (CARS-42) and (2021YFD1200302).

Data availability

The dataset supporting the conclusions of this article is available in Sequence Read Archive (SRA) from the NCBI BioProject, under the accession number PRJNA1171581 (<https://www.ncbi.nlm.nih.gov/sra/>).

Declarations

Ethics approval and consent to participate

This study, which complied with institutional and national guidelines for the care and use of animals, was approved by the Committee of Animal Experiments of the Institute of Animal Sciences, Chinese Academy of Agricultural Sciences (Approval number: IAS2022-103). All efforts were made to minimize animal suffering.

Consent for publication

Not applicable.

Competing interests

The authors declare no competing interests.

Received: 5 November 2024 / Accepted: 5 March 2025

Published online: 28 April 2025

References

- Huang JF, Lin CC. 21 - Production, composition, and quality of Duck eggs. In: Nys Y, Bain M, Van Immerseel F, editors. Improving the safety and quality of eggs and egg products. Woodhead Publishing; 2011. pp. 487–508.
- Chaiyasit W, Brannan RG, Chareonsuk D, Chanasattru W. Comparison of physicochemical and functional properties of chicken and Duck egg albumens. *Braz J Poult Sci.* 2019;21:eRBCA.
- Ligen Z, Qian W, Liping W, Tenghao W, Jing Q, Junbo L, et al. Quality evaluation and lipidomics analysis of salted Duck egg yolk under low-salt pickling process. *Food Chemistry: X.* 2022;16:100502.
- Johnston NP, Jefferies LK, Rodriguez B, Johnston DE. Acceptance of brown-shelled eggs in a white-shelled egg market. *Poult Sci.* 2011;90:1074–9.
- Stefanello C, Santos TC, Murakami AE, Martins EN, Carneiro TC. Productive performance, eggshell quality, and eggshell ultrastructure of laying hens fed diets supplemented with organic trace minerals. *Poult Sci.* 2014;93:104–13.
- Sun K, Ma L, Pan L, Tu K. Sequenced wave signal extraction and classification algorithm for Duck egg crack on-line detection. *Comput Electron Agric.* 2017;142:429–39.
- Widdicombe JP, Rycroft AN, Gregory NG. Hazards with cracked eggs and their relationship to egg shell strength. *J Sci Food Agric.* 2009;89:201–5.
- Drabik K, Karwowska M, Wengerska K, Próchniak T, Adamczuk A, Batkowska J. The variability of quality traits of table eggs and eggshell mineral composition depending on hens' breed and eggshell color. *Animals.* 2021;11:1204.
- Wang H, Ge Y, Zhang L, Wei Y, Li Q, Zhang X, et al. The pigments in eggshell with different colour and the pigment regulatory gene expression in corresponding Chicken's shell gland. *Animal.* 2023;17:100776.
- Jonchère V, Réhault-Godbert S, Hennequet-Antier C, Cabau C, Sibut V, Cogburn LA, et al. Gene expression profiling to identify eggshell proteins involved in physical defense of the chicken egg. *BMC Genomics.* 2010;11:57.
- Wilson PB. Recent advances in avian egg science: A review. *Poult Sci.* 2017;96:3747–54.
- Kennedy GY, Vevers HG. A survey of avian eggshell pigments. *Comp Biochem Physiol Part B: Comp Biochem.* 1976;55:117–23.
- Gorchein A, Lim CK, Cassey P. Extraction and analysis of colourful eggshell pigments using HPLC and HPLC/electrospray ionization tandem mass spectrometry. *Biomed Chromatogr.* 2009;23:602–6.
- Liu H, Hu J, Guo Z, Fan W, Xu Y, Liang S, et al. A single nucleotide polymorphism variant located in the *cis*-regulatory region of the *ABCG2* gene is associated with Mallard egg colour. *Mol Ecol.* 2021;30:1477–91.
- Soledad Fernandez M, Moya A, Lopez L, Arias JL. Secretion pattern, ultrastructural localization and function of extracellular matrix molecules involved in eggshell formation. *Matrix Biol.* 2001;19:793–803.
- Wang X, Zhu P, Sun Z, Zhang J, Sun C. Uterine metabolomic analysis for the regulation of eggshell calcification in chickens. *Metabolites.* 2021;11:575.
- Moan J, Ma L-W, Juzeniene A, Iani V, Juzenas P, Apricena F, et al. Pharmacology of protoporphyrin IX in nude mice after application of ALA and ALA esters. *Int J Cancer.* 2003;103:132–5.
- Rao J, Adams S. 25 - Photodynamic therapy. In: Wolverton SE, editor. Comprehensive dermatologic drug therapy (Fourth Edition). Elsevier; 2021. pp. 280–e2862.
- Kim JH, Choi WJ, Kwon CH, Kil DY. Research note: improvement of eggshell strength and intensity of brown eggshell color by dietary magnesium and δ -aminolevulinic acid supplementation in laying hens. *Poult Sci.* 2022;101:101676.
- Li M, Cai S-Y, Boyer JL. Mechanisms of bile acid mediated inflammation in the liver. *Mol Aspects Med.* 2017;56:45–53.
- Sparks NHC. Eggshell Pigments—from formation to deposition. *Avian Biol Res.* 2011;4:162–7.
- Mahato PL, Weatherby T, Ewell K, Jha R, Mishra B. Scanning electron microscope-based evaluation of eggshell quality. *Poult Sci.* 2024;103:103428.
- Solomon SE. The eggshell: strength, structure and function. *Br Poult Sci.* 2010;51:52–9.
- Zhang Y, Deng Y, Jin Y, Wang S, Huang X, Li K, et al. Age-related changes in eggshell physical properties, ultrastructure, calcium metabolism-related serum indices, and gene expression in eggshell gland during eggshell formation in commercial laying ducks. *Poult Sci.* 2022;101:101573.
- Wang X-T, Deng X-M, Zhao C-J, Li J-Y, Xu G-Y, Lian L-S, et al. Study of the deposition process of eggshell pigments using an improved dissolution method. *Poult Sci.* 2007;86:2236–8.
- Wang XT, Zhao CJ, Li JY, Xu GY, Lian LS, Wu CX, et al. Comparison of the total amount of eggshell pigments in Dongxiang brown-shelled eggs and Dongxiang blue-shelled eggs. *Poult Sci.* 2009;88:1735–9.
- Han GP, Kim JH, Kim J-M, Kil DY. Transcriptomic analysis of the liver in aged laying hens with different eggshell strength. *Poult Sci.* 2023;102:102217.
- Xu W, Mu R, Gegen T, Luo J, Xiao Y, Ou S, et al. Comparative analysis of hepatic transcriptomes and metabolomes of Changshun green-shell laying hens based on different green eggshell color intensities. *Poult Sci.* 2024;103:103220.
- Ito S, Tsudzuki M, Komori M, Mizutani M. Celadon: an eggshell color mutation in Japanese quail. *J Hered.* 1993;84:145–7.
- Taylor D, Walsh M, Cullen A, O'Reilly P. The fracture toughness of eggshell. *Acta Biomater.* 2016;37:21–7.
- Robinson MD, McCarthy DJ, Smyth GK. EdgeR: a bioconductor package for differential expression analysis of digital gene expression data. *Bioinformatics.* 2010;26:139–40.
- Langfelder P, Horvath S. WGCNA: an R package for weighted correlation network analysis. *BMC Bioinformatics.* 2008;9:559.
- Ganger MT, Dietz GD, Ewing SJ. A common base method for analysis of qPCR data and the application of simple blocking in qPCR experiments. *BMC Bioinformatics.* 2017;18:534.
- Ramzan F, Klees S, Schmitt AO, Caverio D, Gúltas M. Identification of Age-Specific and common key regulatory mechanisms governing eggshell strength in chicken using random forests. *Genes.* 2020;11:464.
- Fu Y, Zhou J, Schroyen M, Zhang H, Wu S, Qi G, et al. Decreased eggshell strength caused by impairment of uterine calcium transport coincide with higher bone minerals and quality in aged laying hens. *J Anim Sci Biotechnol.* 2024;15:37.
- Duan G, Liu W, Han H, Li D, Lei Q, Zhou Y, et al. Transcriptome and histological analyses on the uterus of freckle egg laying hens. *BMC Genomics.* 2023;24:738.
- Schreivels MA, Hester PY, Settar P, Moody DE. Identification of quantitative trait loci associated with egg quality, egg production, and body weight in an F2 resource population of chickens1. *Anim Genet.* 2006;37:106–12.
- Mróz E, Michalak K, Orłowska A. Hatchability of Turkey eggs as dependent on shell ultrastructure. *Pol J Nat Sci.* 2007;22:31–42.
- Samiullah S, Roberts J, Chousalkar K. Infectious bronchitis virus and brown shell colour: Australian strains of infectious bronchitis virus affect brown eggshell colour in commercial laying hens differently. *Avian Pathol.* 2016;45:552–8.
- Xu FQ, Li A, Lan JJ, Wang YM, Yan MJ, Lian SY, et al. Study of formation of green eggshell color in ducks through global gene expression. *PLoS ONE.* 2018;13:e0191564.

41. Nie S, Huang Y, Shi M, Qian X, Li H, Peng C, et al. Protective role of ABCG2 against oxidative stress in colorectal cancer and its potential underlying mechanism. *Oncol Rep.* 2018;40:2137–46.
42. Liu L, Zhao T, Shan L, Cao L, Zhu X, Xue Y. Estradiol regulates intestinal ABCG2 to promote urate excretion via the PI3K/Akt pathway. *Nutr Metabolism.* 2021;18:63.
43. Sultan M, Rao A, Elpeleg O, Vaz FM, Abu-Libdeh B, Karpen SJ, et al. Organic solute transporter- β (SLC51B) deficiency in two brothers with congenital diarrhea and features of cholestasis. *Hepatology.* 2018;68:590.
44. Hargitai R, Boross N, Hámori S, Neuberger E, Nyiri Z. Eggshell biliverdin and protoporphyrin pigments in a Songbird: are they derived from erythrocytes, blood plasma, or the shell gland?? *Physiol Biochem Zool.* 2017;90:613–26.
45. Garrod AE. A contribution to the study of uroerythrin. *J Physiol.* 1895;17:438–2.
46. Beruter J, Colombo J-P, Schlunegger UP. Isolation and identification of the urinary pigment uroerythrin. *Eur J Biochem.* 1975;56:239–44.
47. Yamaguchi T, Shioji I, Sugimoto A, Komoda Y, Nakajima H. Chemical structure of a new family of bile pigments from human urine. *J Biochem.* 1994;116:298–303.
48. Weiss M. Über die natur des normalen Gelben Harnfarbstoffs Urochrom und Seine beziehung zum uroerythrin. *Acta Med Scand.* 2009;113:423–43.
49. Bloomer JR. Liver metabolism of porphyrins and haem. *J Gastroenterol Hepatol.* 1998;13:324–9.
50. Bareth B, Dennerlein S, Mick DU, Nikolov M, Urlaub H, Rehling P. The Heme a synthase Cox15 associates with cytochrome C oxidase assembly intermediates during Cox1 maturation. *Mol Cell Biol.* 2013;33:4128–37.
51. Zhou Z, Arroum T, Luo X, Kang R, Lee YJ, Tang D, et al. Diverse functions of cytochrome C in cell death and disease. *Cell Death Differ.* 2024;31:387–404.
52. Jia L, Ma Y, Haywood J, Jiang L, Xue B, Shi H, et al. NPC1L1 deficiency suppresses ileal fibroblast growth factor 15 expression and increases bile acid pool size in High-Fat-Diet-Fed mice. *Cells.* 2021;10:3468.
53. Bomer N, Pavez-Giani MG, Deiman FE, Linders AN, Hoes MF, Baierl CLJ, et al. Selenoprotein DIO2 is a regulator of mitochondrial function, morphology and UPRmt in human cardiomyocytes. *Int J Mol Sci.* 2021;22:11906.
54. Tharehalli U, Svinarenko M, Kraus JM, Kühlwein SD, Szekeley R, Kiesle U, et al. YAP activation drives liver regeneration after cholestatic damage induced by Rbpj deletion. *Int J Mol Sci.* 2018;19:3801.
55. Lu M-Y, Wang W-W, Qi G-H, Xu L, Wang J. Mitochondrial transcription factor A induces the declined mitochondrial biogenesis correlative with depigmentation of brown eggshell in aged laying hens. *Poult Sci.* 2021;100:100811.
56. Samiullah S, Roberts J, Wu S-B. Downregulation of ALA1 by Nicarbazin treatment underlies the reduced synthesis of protoporphyrin IX in shell gland of laying hens. *Sci Rep.* 2017;7:6253.
57. Sah N, Kuehu DL, Khadka VS, Deng Y, Peplowska K, Jha R, et al. RNA sequencing-based analysis of the laying Hen uterus revealed the novel genes and biological pathways involved in the eggshell biomineralization. *Sci Rep.* 2018;8:16853.
58. Lu M-Y, Xu L, Qi G-H, Zhang H-J, Qiu K, Wang J, et al. Mechanisms associated with the depigmentation of brown eggshells: a review. *Poult Sci.* 2021;100:101273.
59. Bar A. Calcium transport in strongly calcifying laying birds: mechanisms and regulation. *Comp Biochem Physiol A: Mol Integr Physiol.* 2009;152:447–69.
60. Liu Z, Sun X, Cai C, He W, Zhang F, Linhardt RJ. Characteristics of glycosaminoglycans in chicken eggshells and the influence of disaccharide composition on eggshell properties. *Poult Sci.* 2016;95:2879–88.
61. Jiang Q, Sun J, He Y, Ma Y, Zhang B, Han Y, et al. Hydroxychloride trace elements improved eggshell quality partly by modulating uterus histological structure and inflammatory cytokines expression in aged laying hens. *Poult Sci.* 2021;100:101453.
62. Fu Y, Wang J, Schroyen M, Chen G, Zhang H, Wu S et al. Effects of rearing systems on the eggshell quality, bone parameters and expression of genes related to bone remodeling in aged laying hens. *Front Physiol.* 2022;13.
63. Li J, Qin Q, Li Y-X, Leng X-F, Wu Y-J. Tri-*ortho*-cresyl phosphate exposure leads to low egg production and poor eggshell quality via disrupting follicular development and shell gland function in laying hens. *Ecotoxicol Environ Saf.* 2021;225:112771.
64. Hu Y, Han J, Ding S, Liu S, Wang H. Identification of ferroptosis-associated biomarkers for the potential diagnosis and treatment of postmenopausal osteoporosis. *Front Endocrinol.* 2022;13.
65. Naik MU, Chen X, Bachman B, Rai G, Maloney D, Jadhav A, et al. Evaluation of two structurally distinct novel inhibitors of apoptosis Signal-Regulating kinase 1 (MAP3K5), as potent Anti-Platelet agents. *Blood.* 2016;128:3833.
66. Nava-Villalba M, Nuñez-Anita RE, Bontempo A, Aceves C. Activation of peroxisome proliferator-activated receptor gamma is crucial for antitumoral effects of 6-iodolactone. *Mol Cancer.* 2015;14:168.
67. Wang J, Yuan Z, Zhang K, Ding X, Bai S, Zeng Q, et al. Epigallocatechin-3-gallate protected vanadium-induced eggshell depigmentation via P38MAPK-Nrf2/HO-1 signaling pathway in laying hens. *Poult Sci.* 2018;97:3109–18.
68. Liang X, Chai B, Duan R, Zhou Y, Huang X, Li Q. Inhibition of FKBP10 attenuates hypertrophic scarring through suppressing fibroblast activity and extracellular matrix deposition. *J Invest Dermatol.* 2017;137:2326–35.
69. Lim J, Lietman C, Grol MW, Castellon A, Dawson B, Adeyeye M et al. Localized chondro-ossification underlies joint dysfunction and motor deficits in the Fkbp10 mouse model of osteogenesis imperfecta. *Proceedings of the National Academy of Sciences.* 2021;118:e2100690118.
70. Qin Y, Zhou Y, Shen Z, Xu B, Chen M, Li Y, et al. WDR62 is involved in spindle assembly by interacting with CEP170 in spermatogenesis. *Development.* 2019;146:dev174128.
71. Malavasi EL, Ghosh A, Booth DG, Zagnoni M, Sherman DL, Brophy PJ. Dynamic early clusters of nodal proteins contribute to node of Ranvier assembly during myelination of peripheral neurons. *eLife.* 2021;10:e68089.
72. Satomoto K, Aoki M, Wakita A, Yamagata H, Mitsumoto T, Okamoto T, et al. Hepatocyte proliferation activity in untreated rats, measured by immunohistochemical detection of Ki-67: the effect of age on the repeated-dose liver micronucleus assay. *Mutat Research/Genetic Toxicol Environ Mutagen.* 2023;890:503658.
73. Liu Y, Xiao J, Cai J, Li R, Sui X, Zhang J, et al. Single-cell immune profiling of mouse liver aging reveals Cxcl2 + macrophages recruit neutrophils to aggravate liver injury. *Hepatology.* 2024;79:589.
74. Han GP, Kim J-M, Kang HK, Kil DY. Transcriptomic analysis of the liver in aged laying hens with different intensity of brown eggshell color. *Anim Biosci.* 2020;34:811–23.
75. Chen Y, Takikawa M, Tsutsumi S, Yamaguchi Y, Okabe A, Shimada M, et al. PHLDA1, another PHLDA family protein that inhibits Akt. *Cancer Sci.* 2018;109:3532–42.
76. Zhou C, Wang R, Cheng D, Zhu Y, Cao Q, Lv W. FLT3/FLT3L-mediated CD103 + dendritic cells alleviates hepatic ischemia-reperfusion injury in mice via activation of Treg cells. *Biomed Pharmacother.* 2019;118:109031.
77. Desterke C, Hasselbalch H, Bordessoule D, Gisslinger H, Vannucchi A, Pierre-Louis O, et al. FLT3 mediated MAPK activation participates in the control of megakaryopoiesis in primary myelofibrosis. *Blood.* 2007;110:1532.
78. Ronjat M, Kiyonaka S, Barbado M, De Waard M, Mori Y. Nuclear life of the voltage-gated Cacnb4 subunit and its role in gene transcription regulation. *Channels.* 2013;7:119–25.

Publisher's note

Springer Nature remains neutral with regard to jurisdictional claims in published maps and institutional affiliations.